Molecular Cancer Research

Inhibiting Integrin β8 to Differentiate and Radiosensitize Glioblastoma-Initiating Cells

Laure Malric[1], Sylvie Monferran[1,2], Caroline Delmas[1], Florent Arnauduc[1,3], Perrine Dahan[1], Sabrina Boyrie[1], Pauline Deshors[1], Vincent Lubrano[3,4], Dina Ferreira Da Mota[3], Julia Gilhodes[5], Thomas Filleron[5], Aurore Siegfried[1,5], Solène Evrard[1,3,5], Aline Kowalski-Chauvel[1], Elizabeth Cohen-Jonathan Moyal[1,3,5], Christine Toulas[1,5], and Anthony Lemarié[1,2]

Abstract

Glioblastomas (GB) are malignant brain tumors with poor prognosis despite treatment with surgery and radio/chemotherapy. These tumors are defined by an important cellular heterogeneity and notably contain a subpopulation of GB-initiating cells (GIC), which contribute to tumor aggressiveness, resistance, and recurrence. Some integrins are specifically expressed by GICs and could be actionable targets to improve GB treatment. Here, integrin β8 (ITGB8) was identified as a potential selective target in this highly tumorigenic GIC subpopulation. Using several patient-derived primocultures, it was demonstrated that ITGB8 is overexpressed in GICs compared with their differentiated progeny. Furthermore, ITGB8 is also overexpressed in GB, and its overexpression is correlated with poor prognosis and with the expression of several other classic stem cell markers. Moreover, inhibiting ITGB8 diminished several main GIC characteristics and features, including self-renewal ability, stemness, migration potential, and tumor formation capacity. Blockade of ITGB8 significantly impaired GIC cell viability via apoptosis induction. Finally, the combination of radiotherapy and ITGB8 targeting radiosensitized GICs through postmitotic cell death.

Implications: This study identifies ITGB8 as a new selective marker for GICs and as a promising therapeutic target in combination with chemo/radiotherapy for the treatment of highly aggressive brain tumors.

Introduction

Glioblastoma (GB, grade IV glioma) is the most frequent and lethal malignant primary adult brain tumor. Surgical resection followed by radio/chemotherapy (30 × 2 Gy and Temozolomide) are the current standard of care. However, prognosis remains extremely poor (median survival of ∼15 months; ref. 1). Recurrences may be notably explained by the strong cellular heterogeneity of these tumors which contain GB-initiating cells (GIC; ref. 2). GICs are characterized by their unlimited self-renew ability, their stem markers overexpression (CD133, Nestin, Olig2, Sox2, Nanog, A2B5, ITGA6...), their multipotent aptitude to differentiate into neural lineages, their localization in perivascular niches, their invasion capacity, their strong radio/chemoresistance, and their higher tumorigenic potential (2). Consequently, GIC targeting represents a strong therapeutic interest in GB.

Among the most considered targets, integrins are the subject of an increasing number of studies. These transmembrane receptors are composed of two noncovalently associated α and β subunits and are key components of the dialogue between cells and their microenvironment. They regulate cell adhesion to extracellular matrix (ECM) or cell surface proteins. They also serve as transmembrane links between extracellular contacts and intracellular cytoskeleton via a bidirectional signaling (inside-out/outside-in; ref. 3). Integrins can then activate pathways leading to gene transcription to sustain proliferation, survival, differentiation, and migration (3, 4). In GB, several integrins have been highlighted in GB progression. αvβ3, αvβ5, and β1 are involved in invasion, angiogenesis, and radioresistance (for review, see ref. 5). α3 (6), α6 (7), α7 (8), and β8 (9) were also reported to be overexpressed in GIC and, particularly for α6 and α7, to be associated with GIC stemness (5). Thus, GIC might express a specific integrin pattern compared with other tumor cells, and some of these integrins may be considered as specific GIC targets. Considering that clinical targeting of αvβ3/αvβ5 integrins in GB patients led to some disappointing results in a recent phase III trial (10), there is an urgent need to identify new targets specific to this GIC population.

β8 integrin (β8) has drawn our attention as a new integrin that may have specific functions in GIC. β8 heterodimerizes with αv and is able to link arginine–glycine–aspartic acid motifs such as in vitronectin, laminin, and latent-TGFβ1/3. β8, expressed in

[1]INSERM UMR 1037, Center for Cancer Research of Toulouse, Toulouse, France. [2]Faculty of Pharmaceutical Sciences, University of Toulouse III Paul Sabatier, Toulouse, France. [3]Faculty of Medicine of Rangueil, University of Toulouse III Paul Sabatier, Toulouse, France. [4]INSERM UMR 1214 - ToNIC, Toulouse, France. [5]IUCT-Oncopole, Toulouse, France.

Note: Supplementary data for this article are available at Molecular Cancer Research Online (http://mcr.aacrjournals.org/).

E. Cohen-Jonathan Moyal, C. Toulas, and A. Lemarié contributed equally to this article.

Corresponding Author: Anthony Lemarié, INSERM UMR 1037, 2 Avenue Hubert Curien, Toulouse 31037, France. Phone: 335-827-41606; E-mail: lemarie.anthony@iuct-oncopole.fr

doi: 10.1158/1541-7786.MCR-18-0386

restrictive cell types including neural stem, neuroepithelial, embryonic, and mesangial renal cells (11, 12), displays a major role in self-renewal and survival of neural progenitor cells (12), and, then, could have a similar function in GIC. Indeed, β8, highly expressed in this GIC subpopulation (9), was preferentially found *in vivo* in GB perivascular and perinecrotic areas (13), some preferential GIC-enriched niches (14). Furthermore, β8 overexpression was also associated with glioma tumor grade (9). Although few studies were conducted in glioma, β8 appears to have a proinvasive role in GB cells (15), whereas it could negatively regulate angiogenesis in transformed human astrocytes (16). In addition, it was recently shown that $\beta8^{HIGH}$-GB cells display several stem characteristics (17). Nevertheless, the effects of β8 targeting on GIC stemness, viability, migration, radioresistance, and tumorigenicity have never been explored.

We hypothesized that β8 could sustain GIC stemness and radioresistance and represent a new GIC-targetable marker. We demonstrated that β8 is overexpressed in GIC and associated with bad prognosis in GB patient cohorts. We highlighted in patient GIC primocultures that β8 is associated *in vitro* and *in vivo* with characteristics and features unique to GIC, including self-renewal ability, stemness status, markers expression, viability, adhesion/migration, radioresistance, and tumorigenesis. We also showed that selective β8 inhibition can impair GIC properties *in vitro* and suppress orthotopic tumor growth *in vivo*. Together, these results identify β8 as a new membrane GIC marker and a potential therapeutic radiosensitizing target.

Materials and Methods

Human tumor collection

The study was conducted on newly diagnosed GB tumor samples isolated from 14 patients. Ten samples were used for IHC studies, and 4 additional GB samples were used to establish 4 primary GIC cell lines (SRA5, SRB1, SRC3, and SB7). For quantitative real-time RT-PCR (qPCR) experiments, additional GIC patient cell lines were also used (A0, C1, D1, G, I, and K). These samples were all obtained after written-informed consent from patients admitted to the Neurosurgery Department at Toulouse University Hospital and processed in accordance with the Institution's Human research Ethics Committee. Tumors used in this study were histologically diagnosed as grade IV astrocytoma according to the World Health Organization criteria.

Cell culture

Ten patient GIC primocultures were established from patient surgical GB samples and were fully characterized either in our previous work (18) or in this study (Supplementary Fig. S1). Briefly, GICs were cultured as GIC-enriched neurospheres (NS) in stem cell medium (SCM), compared with their differentiated counterparts (GB-differentiated cells, GDC), kept in FCS-enriched differentiation medium for at least 15 days, as described (18).

NS generation assays

The related protocol, previously described (18), is detailed in the Supplementary Procedures.

siRNA and shRNA transfection

For siRNA transfection, NS from SRB1 and SRC3 patient cell lines were dissociated and seeded (500,000 cells/well) in 6-well plates before being transfected using Lipofectamine RNAiMAX (Invitrogen) with 3 μL of siRNA [-CTR or -B8-5 or -B8-6 (10 μmol/L; Qiagen)]. Sequences of siRNA were respectively as follows: AATTCTCCGAACGTGTCACGT, AACGTCTATGTCAAATCGACA, and CAGCCTGTTTGCAGTGGTCGA (5′-3′). Cells were harvested for analysis 5 days after transfection. For shRNA transfection, NS from SRB1, SRC3, or SB7 patient cell lines were dissociated and seeded (750,000 cells/well) in 6-well plates before being transfected using Fugene HD (Promega) with 3 μg of shRNA (shRNA-CTR or -B8-1 or -B8-4; Qiagen). For transient transfections, GFP-coupled sequences were used. Cells were then observed by fluorescence microscopy (Nikon), photographed (Camera Coolsnap HQ), and used for experiments. For stable expression, shRNA sequences were coupled with a Neomycin (NEO) resistance gene. Transfected cells were then continuously selected 5 days after transfection with Neomycin (2,000 μg/mL, Merck). Sequences of shRNA-CTR, shB8-1, or shB8-4 were respectively (5′-3′) as follows: GGAATCTCATTCGATGCATAC, CCAAGCTACTTGAGAATATTT, and TCTCGCTCTTGATAGCAAATT.

Western blotting, flow cytometry, and qPCR

The related protocols, previously described (18), are detailed in the Supplementary Procedures. ITGαvβ8 antibody was a gift from Stephen L. Nishimura, University of California, San Francisco, CA (19).

Cell adhesion and migration assays

For adhesion assay, NS cells from SRB1- or SRC3-stable patient cell lines were dissociated, and GICs (50,000 cells in 100 μL/well) were seeded on laminin-coated wells (10 μg/mL; Sigma) in 96-well plates for 6 hours at 37°C. Three random fields per well from triplicate wells were pictured under a 10X objective. Cells were manually delineated. The cell surface (A), perimeter (P), and circularity [$C = 4\pi\ (A/P^2)$] of at least 30 cells per experiment were calculated using Image J software. Cells were classified in two groups: rounded cells with $0.85 < C < 1$; and polarized cells with $0 < C \leq 0.85$. Limits for C were determined by visual identification of a subset of rounded cells as previously described (20). Results are presented as the percentage of polarized cells. For example, if 60 cells have a circularity below or equal to 0.85, and 40 cells have a circularity above 0.85, the percentage of polarized cells is 60%.

For migration assay, transwells (12 wells, BD Biosciences) were precoated in their undersurface with laminin (10 μg/mL). The upper chamber medium consisted of DMEM-F12 only (without EGF/FGF), and the lower chamber medium consisted of SCM. NS from SRB1- or SRC3-stable patient cell lines were dissociated, and GICs (40,000 cells in 500 μL/well) were seeded in Transwells incubated for 24 hours at 37°C. Nonmigrated cells were removed by wiping the membrane upper side with cotton swab. Transmigrated cells were fixed with PFA 4% (ChemCruz) and stained with hematoxylin (Merck). The number of transmigrated cells was counted in at least 3 random fields from duplicate transwells under 10X magnification.

Cell death and clonogenic irradiation assays

SubG1 and Annexin V/propidium iodide (AV/PI) staining, as well as clonogenic irradiation assays, were performed as previously described (18) and detailed in the Supplementary Procedures. Postmitotic cell death was analyzed after cell permeabilization (PBS-0.15% Triton, 5 minutes, room temperature) and DAPI staining (0.2 μg/mL; Sigma). The number of aberrant nuclei observed with DAPI staining was counted in at least 3 random

fields using fluorescence microscopy (Axio-vert). For those three cell death assays, dissociated GICs were treated or not with a 5 Gy irradiation and harvested for analysis 5 days after irradiation (Gamma-cell Exactor 40, Nordion). Finally, Caspase-8 and Caspase-3/7 activity assays were also performed. GICs were dissociated and seeded (20,000 cells in 100 μL/well) on white 96-well plates. Resuspended caspase substrate (Caspase-Glo8 or Caspases-Glo3/7; Promega) was added in each well (100 μL, for 1 hour at 37°C). Caspase activities were quantified by luminometry using a plate reader (FLUOstar Optima). Results show relative caspase activities measured after subtracting the background from all values.

Orthotopic xenograft generation

Nude mice were used in accordance to a protocol (APAFIS#7660-2016110818123504 v2) reviewed and approved by the Institutional Animal Care and Use Committee of Région Midi-Pyrénées (France). This protocol, previously described (18), is detailed in the Supplementary Procedures.

IHC

IHC was performed on paraffin-embedded sections (5 μm) of excised brains of xenografted mice (single staining) or GB patients samples (double staining). The sections were incubated at 57°C for 20 minutes followed by rehydration in xylene and ethanol series. Antigen retrieval was performed at 95°C for 20 minutes using DAKO buffer pH9 (EnVision) and washed with PBS.

For single staining, slides were blocked with Peroxidase Blocking Reagent (EnVision; 5 minutes), washed with PBS, incubated 30 minutes with primary antibodies diluted in antibody diluent (EnVision), and then washed with 0.3% Tween in PBS. The primary antibodies used were rabbit anti-ITGβ8 (Abcam; Ab80673), rabbit anti-Sox2 (Abcam; Ab92494) and mouse anti-Nestin (Millipore; MAB5326). Slides were then incubated with FLEX/HRP (EnVision; 20 minutes), washed (0.3% Tween in PBS), and revealed with DAB (Diaminobenzidine peroxidase buffer) mixed with FLEX/DAB chromogen (EnVision; 5 minutes). Sections were then washed, counterstained with Hemalun of Mayer (Merck), dehydrated, and mounted with Eukitt solution before being viewed on a Nikon microscope. The numbers of positive and total cells were counted in at least 3 random fields under 63X magnification. Results are presented as the average percentage of positive and negative cells for each marker (ITGβ8 or Sox2) in each condition (shCTR or shB8-1 or shB8-4; 4 mice/group).

For double staining, IHC was performed on tumor patients slides ($n = 10$) according to the manufacturer's protocol [EnVision G2 Doublestain System, Rabbit/Mouse (DAB+/Permanent Red)], with rabbit anti-ITGβ8 (Abcam; Ab80673) marked with Permanent Red and mouse anti-Sox2 (Abcam Ab171380) marked with DAB.

The Cancer Genome Atlas and REMBRANDT datasets

We used The Cancer Genome Atlas (TCGA) dataset to analyze gene expression in newly diagnosed primary GB patients (21, 22). For our analyses, a dataset (processed data: version 2015-02-24, downloaded from https://genome-cancer.ucsc.edu) was used based on RNA-seq data (Illumina HiSeq 2000 RNA Sequencing platform, University of North Carolina TCGA genome characterization center, $n = 149$). We first assessed overall survival (OS) using this TCGA dataset among a subgroup of newly diagnosed primary GB patients treated by standard chemo/radiotherapy ($n = 59$). For these analyses, gene expression levels were dichotomized based on a high expression cutoff (within the 75% quartile). We also used the Repository for Molecular Brain Neoplasia Data (REMBRANDT) database ($n = 178$ GB with available survival data) to validate the prognostic ability of ITGB8. Survival rates were estimated by the Kaplan–Meier method with 95% confidence intervals. Univariate analyses were performed using the Log-rank test. We then performed correlation analyses between ITGB8 expression and several classic stem and differentiation genes in the TCGA dataset. Multiple comparisons between molecular subgroups were performed using the Mann–Whitney *U* test. The Benjamini–Hochberg procedure was applied for multiple comparisons. Two-sided *P* values of less than 0.05 were considered statistically significant. Statistical analyses were performed using STATA 12.0 software.

Statistical analysis

All the results depicted in this study are presented as mean ± SEM of at least three independent experiments in the same cell line and were reproduced in at least 1 or 2 other cell lines. Significant differences (*, $P < 0.05$; **, $P < 0.01$; and ***, $P < 0.001$) were evaluated with the unpaired Student *t* test. The Log-rank analysis of Kaplan–Meier survival curves was used to evaluate the tumorigenesis of injected cells, with $P < 0.05$ considered as significantly different (**, $P < 0.01$ and ***, $P < 0.001$).

Results

ITGβ8 is overexpressed in GIC

As we hypothesized a specific integrin expression pattern in GIC, we screened at the RNA level the expression of a panel of integrins in 10 patient GIC-enriched NS cell lines, fully characterized either in our previous work (18) or in this study (Supplementary Fig. S1A). All stem markers (Olig2, Sox2, A2B5) appeared overexpressed in all GIC compared with the corresponding GDCs, which contrarily overexpressed differentiation markers (neuronal TUJ1, astrocytic GFAP; Supplementary Fig. S1B–S1D). We then analyzed mRNA and protein expressions of main integrins in GIC and GDC (Supplementary Fig. S2). Briefly, ITGα6 was overexpressed in GIC, as previously shown (7). ITGβ3 displayed a similar pattern, but at varying degrees according to the cell line. Contrarily, ITGβ5 and ITGβ1 appeared to be restricted to the GDC cell surface, as well as ITGβ4 in GDC total protein extracts. ITGαv protein was, for its part, equally expressed in both GIC and GDC. However, we noticed that ITGβ8 mRNAs were upregulated in all GICs compared with their differentiated progeny (Fig. 1A) and compared with adult healthy neural tissues, neural stem cells, or related GDC (Fig. 1B). Moreover, we confirmed in 4 patient cell lines (SRA5, SRB1, SRC3, and SB7) that β8 protein was also overexpressed in GIC compared with their GDC counterparts, as well as in whole cell lysates by Western blot (Fig. 1C) and at the membrane cell surface by FACS analysis of both β8 and αvβ8 (Fig. 1D). Based on these results, we focused our study on ITGβ8, which appeared, as ITGα6 (7), to be selectively expressed at the GIC membrane and barely present in GDC.

Expression levels of ITGβ8 and stem markers are correlated in GB patients

As β8 seemed to be selectively expressed in GIC, we performed statistical correlation analysis between ITGB8 expression and stem (NG2, GLI1, MSI1, NANOG, NESTIN, NOTCH1, SOX2,

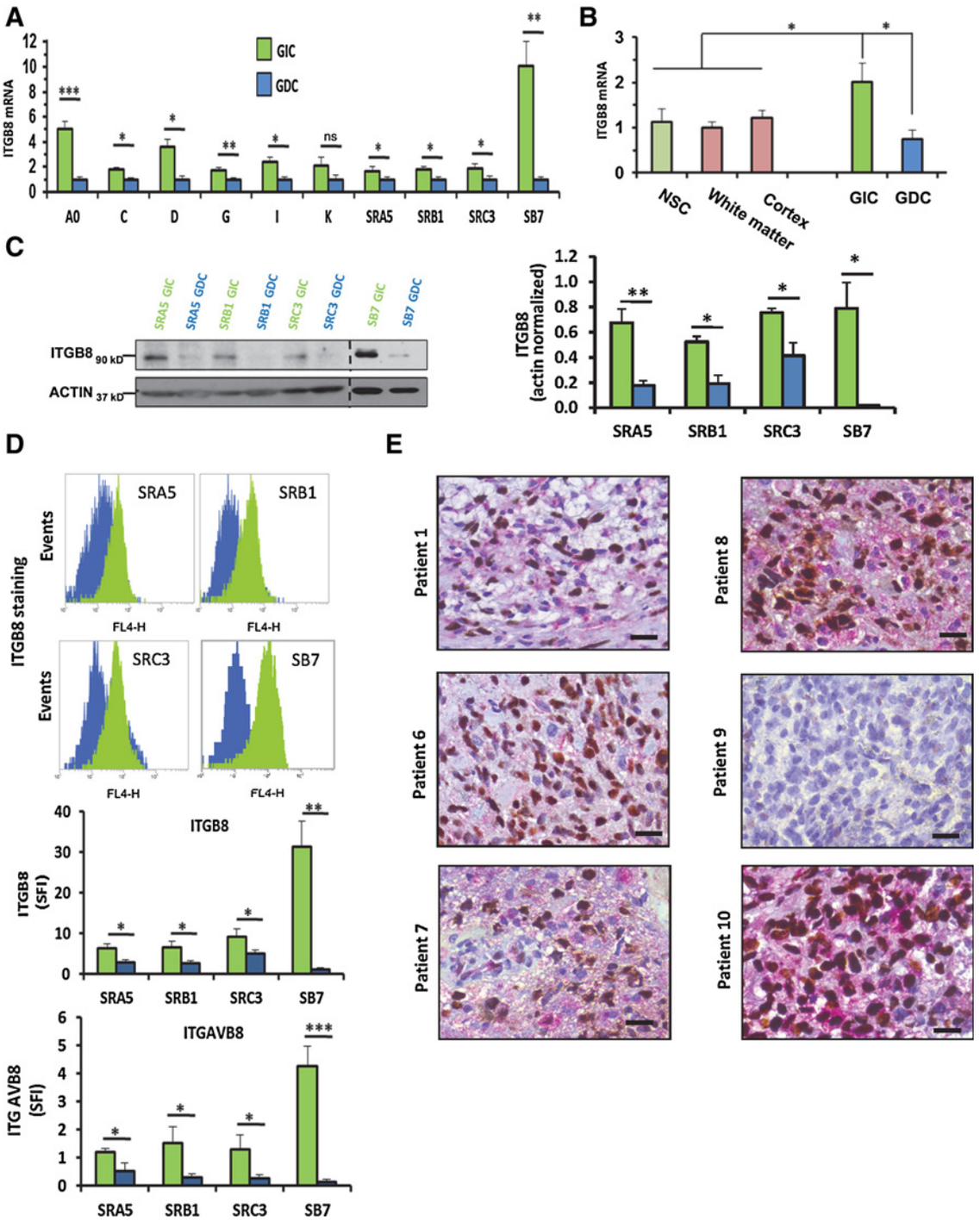

Figure 1.

ITGβ8 is overexpressed in GB and particularly in GIC compared with GDC. **A–D,** GIC-enriched NS cell lines isolated from 10 patient tumors were maintained in stem cell medium or allowed to differentiate as adherent GDC for 15 days in FCS-enriched medium. **A,** *ITGB8* mRNA levels in GIC and related-GDC determined by RT-qPCR. Shown are the fold inductions expressed as mean ± SEM of at least three independent experiments (normalized to GDC expression). ns, nonsignificant; *, $P \leq 0.05$; **, $P \leq 0.01$; and ***, $P \leq 0.001$. **B,** ITGβ8 mRNA levels in GIC, in related GDC, and in human healthy samples [neural stem cells (NSC), white matter and cortex] determined by RT-qPCR. *ITGB8* mRNA levels in the white matter sample were used as a reference of normal brain expression. Shown are the fold inductions expressed as mean ± SEM of at least three independent experiments. *, $P \leq 0.05$. **C,** Immunoblot analysis of the ITGβ8 expression in GIC and related GDC (left). Blots were representative of at least 3 independent experiments in 4 patient cell lines (SRA5, SRB1, SRC3, and SB7) and were then quantified and normalized with actin (right). *, $P \leq 0.05$ and **, $P \leq 0.01$. **D,** Immunofluorescence analysis performed by FACS for membrane ITGβ8 (top) and ITGαvβ8 (bottom) expression. For ITGβ8, representative FACS plot overlays were depicted for all cell lines. The Specific Fluorescence Index (SFI), used to evaluate the marker expression level, was expressed as mean ± SEM of at least three independent experiments. *, $P \leq 0.05$; **, $P \leq 0.01$; and ***, $P \leq 0.001$. **E,** Immunohistochemical colocalizations of ITGβ8 (Permanent Red) and Sox2 (DAB) in GB biopsies. Shown are the representative microphotographs of $n = 6$ of 10 patient biopsies. Magnification, ×63; scale bar, 50 μm.

SHH, PROM1, ITGA6, OLIG2, and CD44) and differentiated (GFAP, MAP2, TUJ1, MAL, OMG) markers in TCGA database ($n = 146$ GB patients). We observed a significant positive correlation of ITGB8 with all the stem markers tested, except PROM1 and OLIG2 (Supplementary Table S1; Supplementary Fig. S3A). In contrast, β8 negatively correlated with neuronal markers (MAP2, TUBB3, and HRNBP3/NeuN) and oligodendrocytic markers (MAL and OMG; Supplementary Table S1; Supplementary Fig. S3B). To further study the link between β8 and stem markers, we analyzed the expression of ITGβ8 and Sox2 by IHC double-staining in GB patients cohort ($n = 10$) for both ITGβ8 and Sox2 (Fig. 1E; Supplementary Fig. S4A). Patients that did not express Sox2 (2–5 and 9) also failed to express β8 (Fig. 1E; Supplementary Fig. S4B). Contrarily, patients that were positive for Sox2 (1, 6–8, and 10) also expressed β8 at varying degrees. Importantly, β8-stained cells appeared to be positive for Sox2 as well (Fig. 1E). Altogether, these results showed that ITGβ8 is selectively expressed by GIC *in vitro* and that ITGβ8-positive cells in GB patients are also Sox2-positive.

ITGβ8 inhibition alters GIC stemness

We subsequently designed shRNA and siRNA strategies to selectively downregulate β8 and assess its functions in GIC. Two GFP-coupled β8-targeting shRNA sequences (shB8-1/-4) and a negative control (shCTR) were used to transiently transfect NS-dissociated cells for 7 days. We observed in SRB1 and SRC3 GIC cultures that shB8s potently inhibited ITGβ8 expression at mRNA and protein levels, particularly at the cell membrane, compared with shCTR condition (Fig. 2A–C). For stable inhibition, SRB1 and SRC3 GIC were transfected with the same shRNA sequences coupled to a neomycin-resistance gene and then G418-selected to establish stable cell lines. These stable NS cell lines displayed a significant inhibition for ITGβ8 mRNA and protein expression (Fig. 2D and E). A similar effect was observed after GIC transfection for 5 days with two β8-targeting siRNAs (siB8-5/-6) compared with a control siRNA (siCTR; Supplementary Fig. S5A–S5C). Finally, as integrins are mainly known as key players in adhesion and migration processes, both largely activated in GIC (5, 23), we consequently performed GIC adhesion assays on laminin, a known β8 substrate (24), to validate the functional consequences of ITGβ8 targeting. We demonstrated that stable shβ8 transfection decreased the cell adhesion and spreading rates, with a reduction of both cell area and polarization compared with shCTR (Fig. 2F). We also assessed GIC migration by seeding stable shB8 or shCTR cells (SRB1/SRC3) on laminin-coated transwells for 24 hours. ITGβ8 knockdown reduced migration rate by 30% to 50% compared with shCTR (Fig. 2G). Collectively, these results show that our interference RNA strategies to inhibit ITGβ8 can potently block both protein expression and fundamental functions of this integrin in GIC.

The self-renewal ability in limiting dilution condition, a major stem characteristic, was then assessed by evaluating the NS-forming capacity of SRB1/SRC3 GIC at low cell density after β8 targeting. After transient transfection, $GFP^+/ITG\beta8^-$ population isolated from shB8 GIC displayed a dramatically lower ability to form NS compared with the $GFP^+/ITG\beta8^+$ population sorted from shCTR GIC (Fig. 3A). Moreover, stable GIC transfection with shB8-1/-4 induced a similar decrease of the NS generation ability (Fig. 3B and C), with, in some cases, the appearance of an adherent phenotype potentially compatible with a more differentiated state (Fig. 3B). This major alteration of the *in vitro* GIC self-renewal ability after ITGβ8 inhibition can be mediated by several processes, notably by an impairment of their stem phenotype. Indeed, we observed in SRB1/SRC3 GIC a noticeable decrease (~5% to 15%) of the GIC subpopulation within the NS structures in response to ITGβ8 inhibition after either transient or stable transfection (Fig. 4A and B). Moreover, the transient transfection of shB8s induced a significant decrease of Olig2 and Nestin stem markers and an increase of the differentiation markers TUJ1 (neuronal) and MAL (oligodendrocytic) at the mRNA level (Fig. 4C). By Western blot, we confirmed the decrease of these stem markers in favor of an increase of TUJ1/OMG differentiation proteins after ITGβ8 inhibition (Fig. 4D). These variations in stem (Sox2, Nestin, and ITGA6) and differentiation (GFAP, OMG, MAL, and O4) markers were also found in GIC stably depleted for β8 at mRNA and protein levels (Fig. 4E and F). In addition, siRNA-mediated β8 inhibition (siB8-5/-6) was also associated with a strong downregulation of stem markers (Sox2, Nestin, NG2, and Olig2) and an upregulation of differentiation markers (TUJ1, MAL, or OMG) at the mRNA and protein levels, in 5-day–transfected SRB1/SRC3 GIC (Supplementary Fig. S5D and S5E). Altogether, these results suggest that ITGβ8 knockdown induces a differentiation process in GIC and an alteration of their stemness characteristics.

ITGβ8 inhibition decreases GIC viability and induces apoptosis

As an impairment of GIC self-renewal ability could also be linked to viability alteration, we analyzed subG1 population after GIC transient transfection with β8-shRNAs. We demonstrated that this subpopulation was significantly increased compared with shCTR GIC cells (Fig. 5A). We hypothesized that this viability loss may be associated with the induction of a proapoptotic mechanism. We observed by qPCR that GIC transient transfection with shB8s induced a decrease of Bcl2 and Survivin, two anti-apoptotic genes, and an increase of Bax/Bcl2 ratio (Fig. 5B). These transcriptional data were confirmed by Western blot as we noticed an increase of effector Caspases-3/7 and PARP cleavages, an overexpression of the proapoptotic protein Bax, and a down-regulation of the antiapoptotic protein Bcl2 (Fig. 5C). To fully describe this apoptotic process, we measured caspase activities and found a significant increase in Caspases-3/7 activity in SRB1 and SRC3 GIC cell lines (Fig. 5D). Interestingly, we similarly observed a reduction of Bcl2 and Survivin mRNAs and an increase in Caspases-3/7 activity in cells transfected with ITGβ8-targeting siRNAs (Supplementary Fig. S5F and S5G). Of note, we also noticed with siβ8 a significant activation of initiator Caspase-8. Altogether, these results suggest that ITGβ8 knockdown induces in GIC, in addition to their differentiation, the induction of an apoptotic process.

ITGβ8 targeting mediates GIC radiosensitization

Our results show that ITGβ8 can support in GIC several major *in vitro* mechanisms, such as prosurvival processes, stemness maintenance, and proadhesive/migratory properties. We hypothesized that β8 inhibition in clinic could contribute to sensitize GIC, strongly chemo/radioresistant (2, 25), to conventional therapies. Thus, we studied the combined effects of ITGβ8-stable inhibition and ionizing radiations (IR) on GIC. We treated shB8-stable GIC clones (SRB1/SRC3) with IR (5 Gy) and observed, 4 days after irradiation, that ITGβ8 targeting significantly increased the percentage of subG1 (Fig. 6A) and

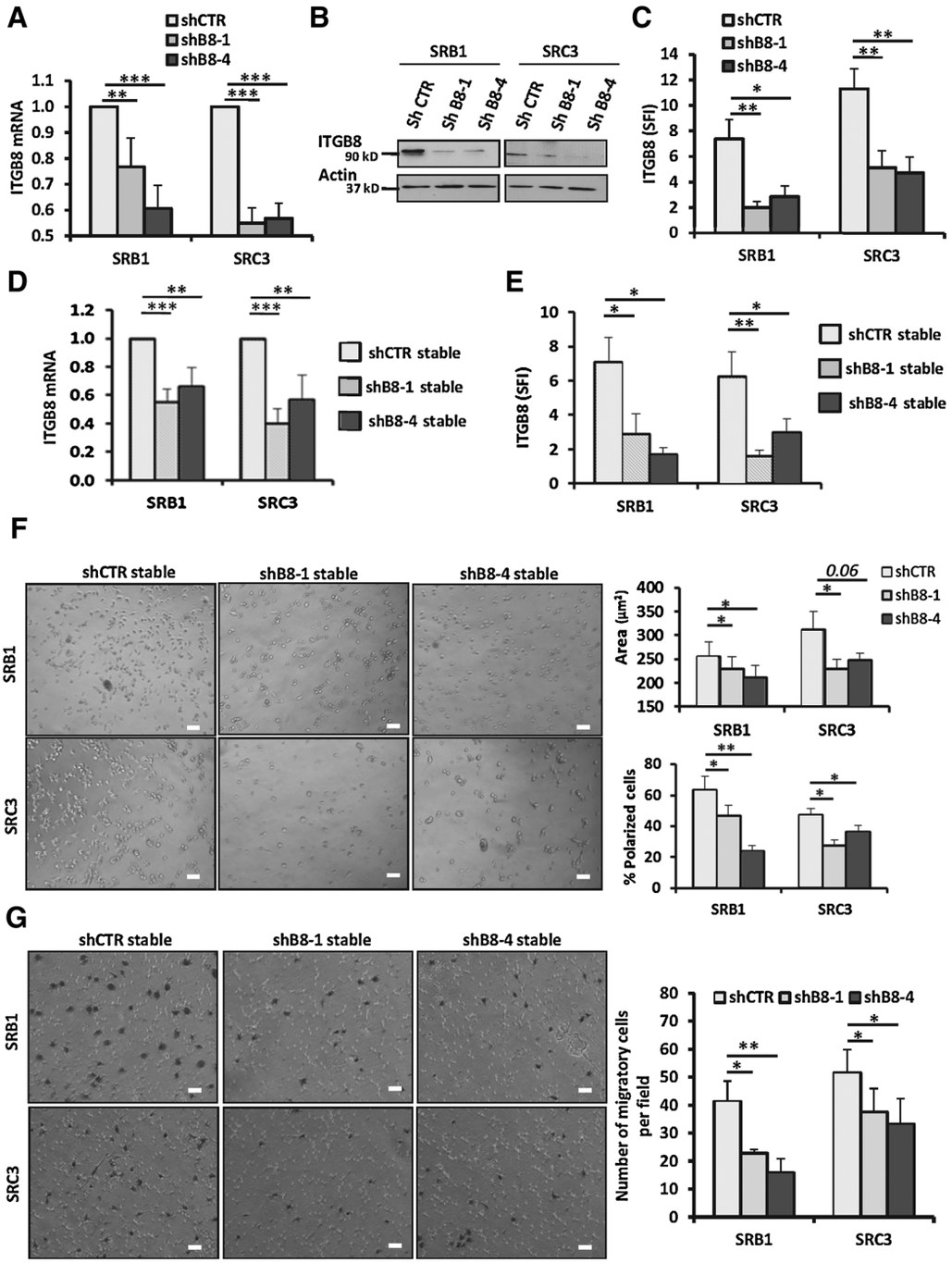

Figure 2.

ITGβ8 is efficiently downregulated in GIC by specific shRNA and siRNA. **A–C,** GIC-enriched NS cells isolated from 2 patient tumors (SRB1 and SRC3) were transfected with 2 different ITGβ8-targeting shRNA (shB8-1 or -4) or with a negative control shRNA (shCTR). Seven days after transfection, ITGβ8 expression levels were then analyzed in NS cells at the mRNA level by RT-qPCR (**A**) or at the protein level either by Immunoblot (**B**) or FACS (**C**). Results are expressed as the mean ± SEM of at least three independent experiments. *, $P \leq 0.05$; **, $P \leq 0.01$; and ***, $P \leq 0.001$ compared with the control condition (shCTR). **D–G,** SRB1 and SRC3 GIC previously transfected with shRNAs (shB8-1, shB8-4, or shCTR) expressing the neomycin-resistance gene were then selected by G418 during at least 20 days in order to establish stable cell lines. ITGβ8 expression levels were then analyzed at the mRNA level by RT-qPCR (**D**) or at the protein level by FACS (**E**). Stably-transfected GIC cell lines were also dissociated and submitted to (**F**) adhesion or (**G**) migration assays. **F,** Cells were seeded on laminin, then allowed to spread for 6 hours. Phase contrast photomicrographs of cells at magnification of ×10; scale bar, 6 µm (left). Quantification of area and percentage of polarized cells (right). In each experiment, the cell surface and the percentage of polarized cells of at least 30 individual cells were analyzed as described in the Material and Methods section. Three independent experiments were performed in duplicate. **G,** Cells were seeded in the upper reservoir of Transwells coated on their undersurface with laminin. Phase contrast photomicrographs of migratory cells 24 hours after seeding. Magnification, ×10; scale bar, 6 µm (left). Migration was quantified by counting Hemalun-stained cells (right). **D–G,** Results are expressed as the mean ± SEM of at least three independent experiments. *, $P \leq 0.05$; **, $P \leq 0.01$; and ***, $P \leq 0.001$ compared with the related control condition (shCTR).

apoptotic AV-positive cells (Fig. 6B), compared with shCTR cells. In addition, the postmitotic cell death, a common death mechanism observed in cancer cells after irradiation and characterized by the presence of giant multinucleated cells and micronuclei (26), appeared also significantly increased in irradiated shB8s (Fig. 6C). To fully demonstrate the radiosensitizing effect of ITGβ8 downregulation in GIC, we performed clonogenic assays at low cell density and measured the NS generation potential of shCTR or shB8s stably-transfected GIC (SRB1/SRC3) in response to increasing IR doses (0–10 Gy). We observed that in response to IR, ITGβ8 silencing led to a significant decrease in the NS-surviving fraction compared with shCTR condition (Fig. 6D). Altogether, ITGβ8 inhibition appears to radiosensitize GIC for cell death induction.

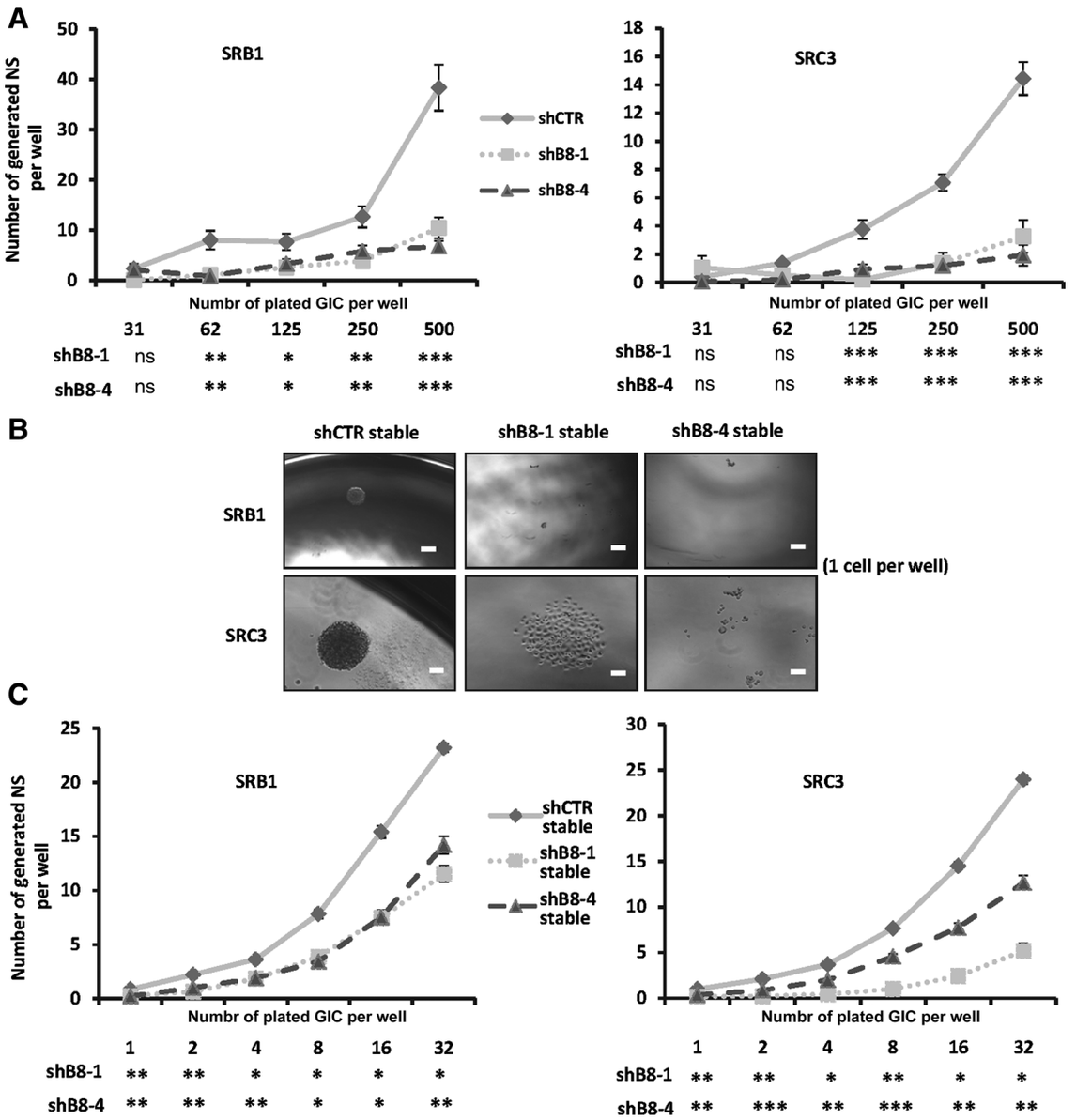

Figure 3.

ITGβ8 knockdown decreases GIC self-renewal. **A,** SRB1 and SRC3 GICs were transfected with GFP-expressing shB8-1, sB8-4, or shCTR. Four days after transfection, GFP-positive GICs were subjected to FACS sorting of either ITGB8^{+} or ITGB8^{-} GIC for the shCTR or the shB8 conditions, respectively. The sorted GICs were then plated in 96-well plates at low-cell densities (31 to 500 cells/well) to study their ability to generate primary NS through limiting dilution assays. **B** and **C,** A similar limiting dilution assay at lower densities (1 to 32 cells/well) was performed in SRB1- and SRC3-stable cell lines to assess the secondary NS forming ability of GIC transfected with shB8-1, sB8-4, or shCTR. **B,** Phase contrast photomicrographs of the NS generated at the density of 1 cell per well. Magnification, ×10; scale bar, 6 μm. **A** and **C,** Results are expressed as the mean ± SEM of at least three independent experiments. *, $P \leq 0.05$; **, $P \leq 0.01$; and ***, $P \leq 0.001$ compared with the related shCTR condition.

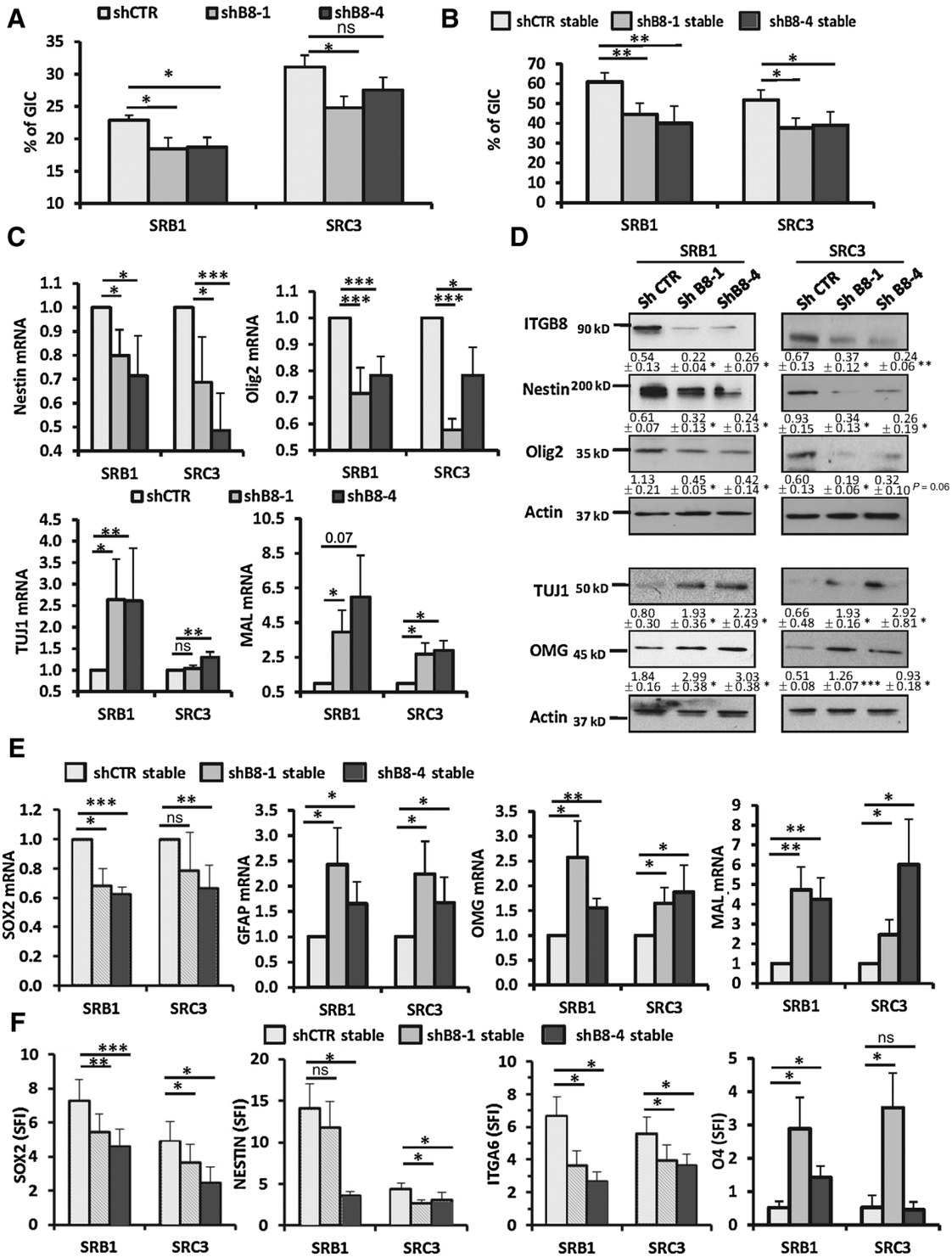

Figure 4.

ITGβ8 knockdown decreases GIC stemness. **A** and **B,** FACS analysis of the percentage of the GIC population (as described in ref. 18) on transfected cells, either 4 days after transfection of GIC (SRB1 and SRC3) with shB8-1, shB8-4, or shCTR (**A**) or on stably-transfected GIC cell lines (SRB1 and SRC3) with shRNAs (shB8-1, shB8-4, or shCTR; **B**). **C–F,** Expression levels of stem markers (Nestin, Olig2, Sox2, and ITGA6) and differentiation markers (GFAP, TUJ1, O4, MAL, and OMG) were analyzed in GICs at the mRNA level by RT-qPCR (**C** and **E**) or at the protein level either by Immunoblots (**D**) or by FACS immunofluorescence (**F**). GICs (SRB1 and SRC3) were transfected with shB8-1, shB8-4, or shCTR for 4 days (**C**) or 7 days (**D**), or were stably transfected with shRNAs (shB8-1, shB8-4, or shCTR; **E**). In **D**, blots were quantified (Image J software), and the ratios relative to the corresponding Actin loading control were calculated. The mean ± SEM of at least three independent experiments were indicated under each blot. **A–F,** Results are expressed as the mean ± SEM of at least three independent experiments. *, $P \leq 0.05$; **, $P \leq 0.01$; and ***, $P \leq 0.001$ compared with the related shCTR condition.

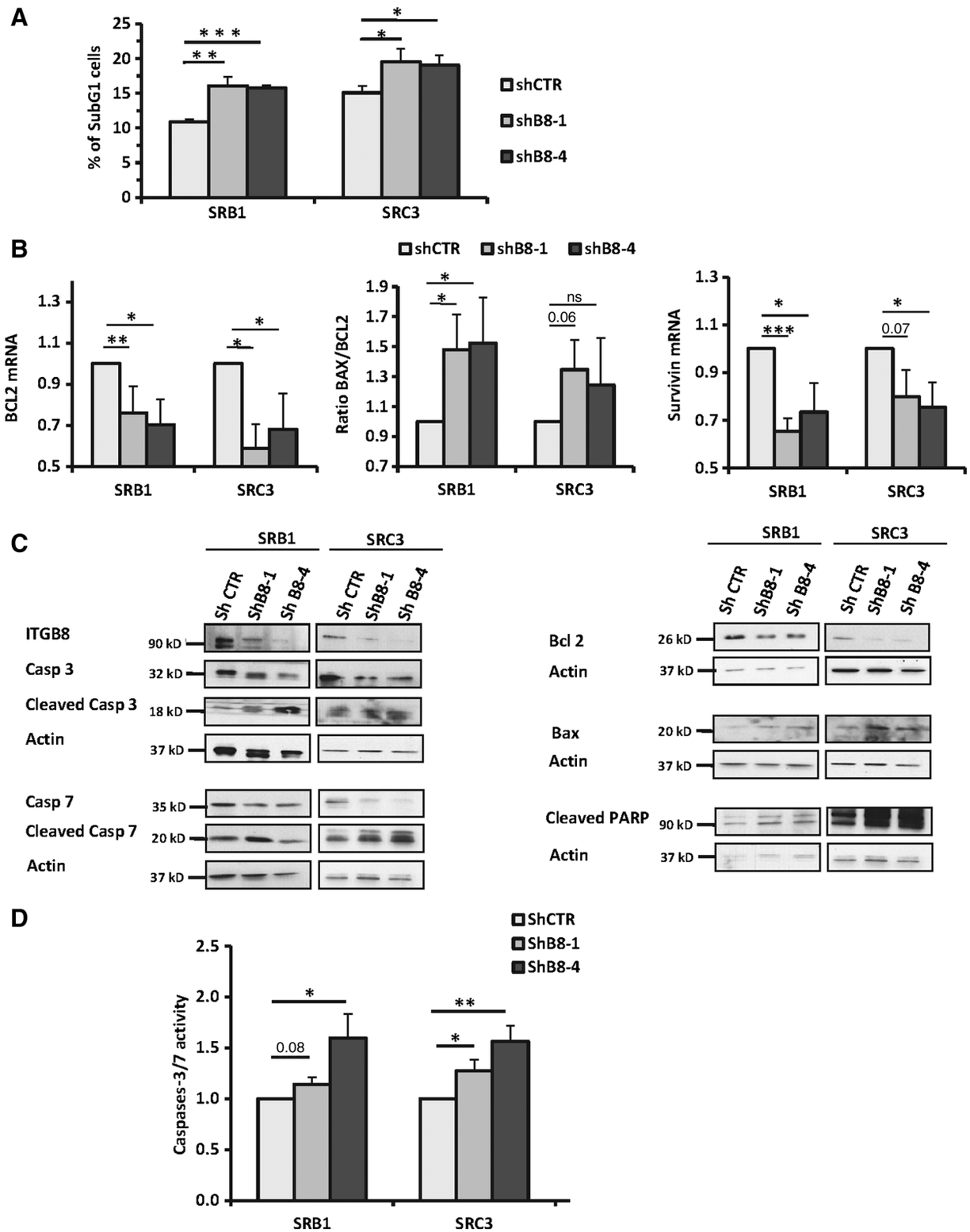

Figure 5.

ITGβ8 knockdown induces GIC apoptosis. **A–D,** SRB1 and SRC3 GICs were transfected with shB8-1, shB8-4, or shCTR and were harvested 7 days after transfection. GICs were subjected to: subG1 analysis by FACS (**A**), RT-qPCR analysis of cell death markers (BCL2, BAX, and Survivin; **B**), immunoblots of cell death markers (Caspase-3, Caspase-7, BCL2, BAX, and PARP; **C**), or Caspase-3/7 activity assays (**D**). **A–B** and **D,** Results are expressed as the mean ± SEM of at least three independent experiments. *, $P \leq 0.05$; **, $P \leq 0.01$; and ***, $P \leq 0.001$ compared with the related shCTR condition.

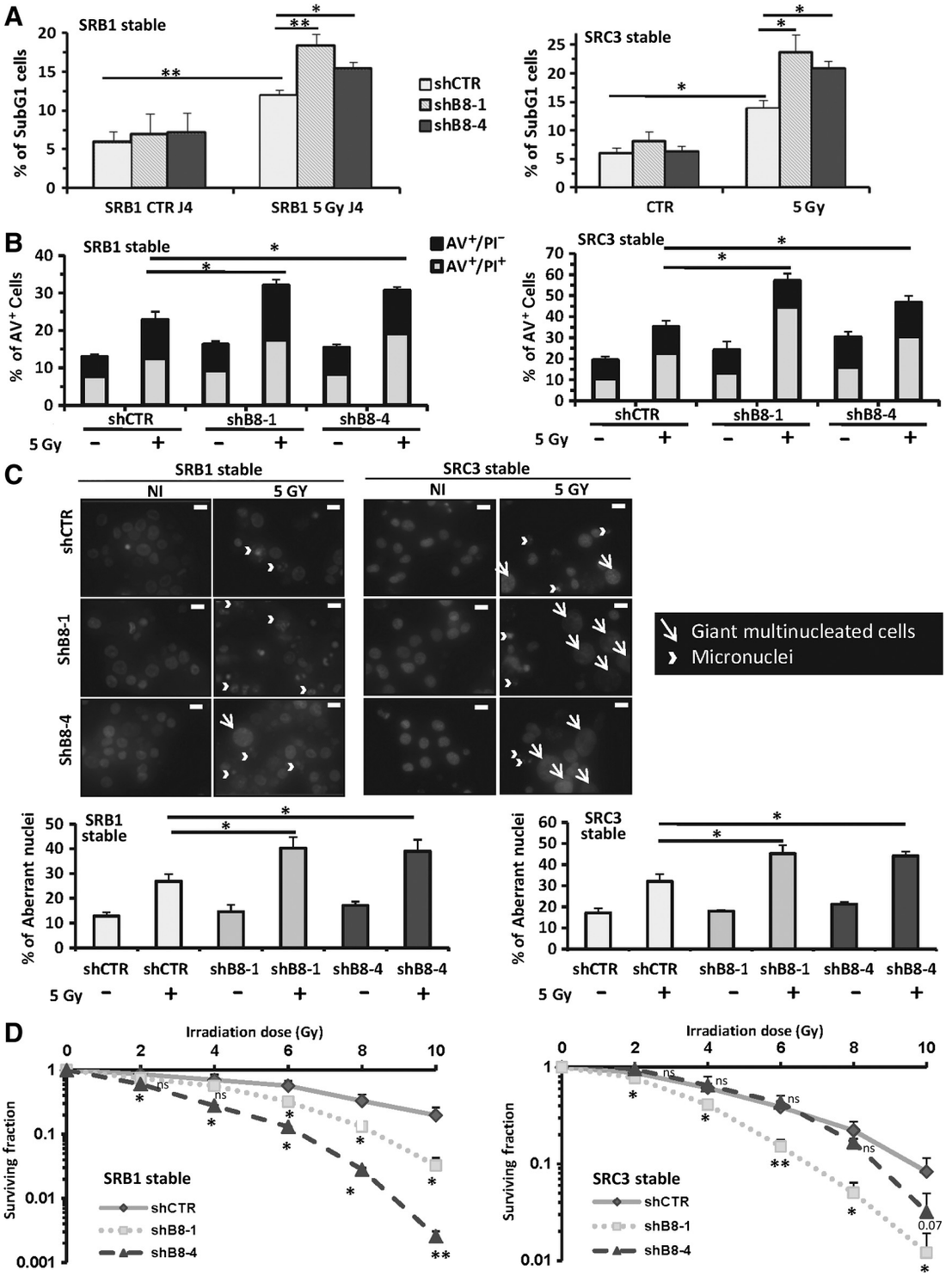

Figure 6.

ITGβ8 knockdown radiosensitizes the GIC population. **A–D,** Stably-transfected (shB8-1, shB8-4, or shCTR) SRB1 and SRC3 GIC cell lines were dissociated and irradiated at the indicated dose. **A–C,** Five days after a 5-Gy irradiation, cells were subjected to either (**A**) subG1 analysis by FACS, (**B**) AV/PI double staining by FACS, or (**C**) postmitotic cell death assay. In the latter case, some representative DAPI photomicrographs are presented. Magnification, ×20; scale bar, 12 μm. **D,** Prior to irradiation (2, 4, 6, 8, or 10 Gy), stably-transfected NS were dissociated and plated in 96-well plates (500 cells/well) in order to determine the surviving fraction by clonogenic assay. The number of growing NS clones was determined by microscopy 10 days after irradiation. **A–D,** Results are expressed as the mean ± SEM of at least three independent experiments. *, $P \leq 0.05$; **, $P \leq 0.01$; and ***, $P \leq 0.001$ compared with the related shCTR condition.

ITGβ8 expression is associated to GIC tumorigenicity and patient worse prognosis

To further explore β8 functions in GB cells stemness *in vivo*, we analyzed the tumorigenic potential of ITGβ8-downregulated GIC in orthotopically xenografted nude mice. All the three mice groups (shCTR/shB8-1/shB8-4) experienced, at different time points, some neurologic signs and displayed, after autopsy, Nestin-positive–invasive brain tumor areas (Fig. 7A). However, we noticed a significant survival advantage for mice xenografted with shB8-4 SRB1 GIC compared with shCTR, and a similar tendency with shB8-1 (Fig. 7B). We then analyzed by IHC both β8 and Sox2 expression patterns in tumor areas of xenografted mice and noticed a marked decrease of both ITGB8- and Sox2-positive cells (from 60%–70% to 10%–20%) in shB8s subgroups compared with shCTR (Fig. 7C). As β8 inhibition appeared to decrease the GIC tumorigenicity, we hypothesized that low ITGβ8 expression could confer to GB patients a survival advantage after standard chemoradiotherapy. Using TCGA, we determined patient OS according to ITGB8 expression on a specific group of newly diagnosed primary GB solely treated with standard chemoradiotherapy ($n = 59$). In this particular population, β8 overexpression was significantly associated with OS decrease ($P = 0.033$), from 21.3 ($\beta8^{LOW}$) to 14.5 months ($\beta8^{HIGH}$; Fig. 7D). REMBRANDT GB dataset (primary GB with survival data, $n = 177$) confirmed (Fig. 7E) that ITGB8 overexpression is associated with a reduced OS, as previously reported in a larger REMBRANDT cohort of low- and high-grade gliomas ($n = 339$; ref. 15). Interestingly, we showed in the REMBRANDT GB cohort that ITGB8 is significantly overexpressed in GB compared with normal brain tissues and with lower-grade astrocytomas and oligodendrogliomas, both associated to a better prognosis than GB (Fig. 7F; ref. 27). Eventually, ITGB8 expression is associated *in vivo* to a reduced survival in GIC-xenografted mice, and its overexpression in GB patients, positively correlated with a large panel of stem markers (Fig. 1E), is linked to a worse prognosis in two independent GB cohorts.

Discussion

Despite intense efforts to understand GB-malignant processes and identify new druggable targets, it must be noted that prognostic and therapeutic protocols have not changed since more than a decade. To improve GB patient's outcome, current researches mostly focus on GIC biology to specifically target these tumorigenic stem-like cells and overpass their resistance mechanisms. In line with this, our study identifies β8 integrin as a new GIC functional marker and highlights for the first time its potential therapeutic interest for GB radiosensitization.

We first demonstrated in GB patient primocultures that β8 is strongly overexpressed at the GIC surface. We also highlighted a stronger β8 expression in GIC compared with their differentiated counterparts, as already suggested in GB cells (9, 17), but also in colorectal cancer cells (28). In addition, we analyzed TCGA database and found that β8 expression in GB samples is correlated positively with the expression of numerous stem markers and negatively with neural differentiation markers. We also performed IHC costaining of the stem-factor Sox2 and β8 in several patient GB biopsies and demonstrated that β8-positive cells were also positive for Sox2 (Fig. 1). Altogether, these elements are in favor of a more selective β8 expression in GIC. Interestingly, GICs were proved *in vivo* to reside in perivascular niches (14), and several works described indeed a positive correlation of β8-stained cells with perivascular areas in primary GB patient's samples (13, 17). Besides, we previously showed that ITGβ8 is significantly overexpressed in the Classical molecular GB subtype, compared with Mesenchymal and Proneural subtypes in the Verhaak's molecular classification (5). Actually, this Classical subtype was characterized through single-cell molecular analysis by a notable stemness signature (29) and was shown to overexpress ITGα6 and ITGα7, two other GIC-associated integrins (7, 8). Finally, it was recently shown in GB patient tumor bulks that $\beta8^{HIGH}$-sorted cells were defined by a superior self-renewal ability *in vitro* and an increased tumorigenicity *in vivo*, two major GIC properties (17). It could be concluded from our results and these observations that ITGβ8 may be used as a new biomarker to detect and, possibly, enrich GIC from the tumor mass.

Furthermore, several studies measured β8 protein expression in tumor samples obtained from large patient cohorts and reported a rather specific expression of β8 in tumor cells, much higher than in tumor endothelial cells and healthy brain tissues (30, 31). In this context, β8 expression was shown to positively correlate with the glioma grade, with a higher expression in grade IV GB (9, 30). To go further, using TCGA and REMBRANDT databases, we demonstrated that β8 is upregulated in GB compared with healthy tissues (5) and that a high β8 level is associated with a worse prognosis in GB patients (Fig. 7). Consequently, it would be of great interest in clinic to take advantage of this new GIC biomarker as a potential prognostic marker. Of note, this new prognostic biomarker may be used in combination with other integrins previously described as prognostic factors in GB, such as α5 (32), β1 (33), and αvβ3 (34).

Besides the potential of ITGβ8 as a new biomarker to detect GIC in tumor mass and to assess GB aggressiveness, we hypothesized that this particular integrin could be an attractive target to specifically impair GIC functions. To this end, we demonstrated that β8 silencing by interference RNA in GIC resulted *in vitro* in a strong decrease of their NS formation ability (Fig. 3), linked to their self-renewal property, and of cell adhesion and migration capacities (Fig. 2), some key features sustaining GIC invasion and tumorigenesis (35). These effects were correlated with a global increase of GIC differentiation pattern in response to β8 downregulation (Fig. 4). In this respect, stable β8 targeting significantly delayed the growth of GIC-derived orthotopic xenografts and improved nude mice survival, with a major decrease of Sox2 staining in β8-negative tumors (Fig. 7). Interestingly, the β8 role in stem markers maintenance and in self-renewal was previously evoked in murine NPC (12) and in sorted-$\beta8^{HIGH}$ GB cells isolated from tumors (17). In this study, the $\beta8^{LOW}$ population was also shown to be less tumorigenic in orthotopically xenografted nude mice, confirming our *in vivo* results. Besides that, GICs also display high capacities for migration/invasion (23, 36), and we demonstrated here that β8 supports GIC-adhesive and -migratory properties. Interestingly, β8 was previously described to sustain proinvasive ability in GB cells and to increase the migration of transformed human astrocytes via TGFβ activation (15, 16). Moreover, β8 was shown to promote motility of prostatic tumor cells (37) and to favor a MMP-9/-2–dependent proadhesive/prometastatic process in human lung cancer cells (38). Altogether, we showed that β8 inhibition in GIC could mediate the differentiation of these tumor cells and the loss of their stem-associated properties. Although the precise mechanisms of these alterations need to be deciphered, therapeutic strategies should take advantage of this

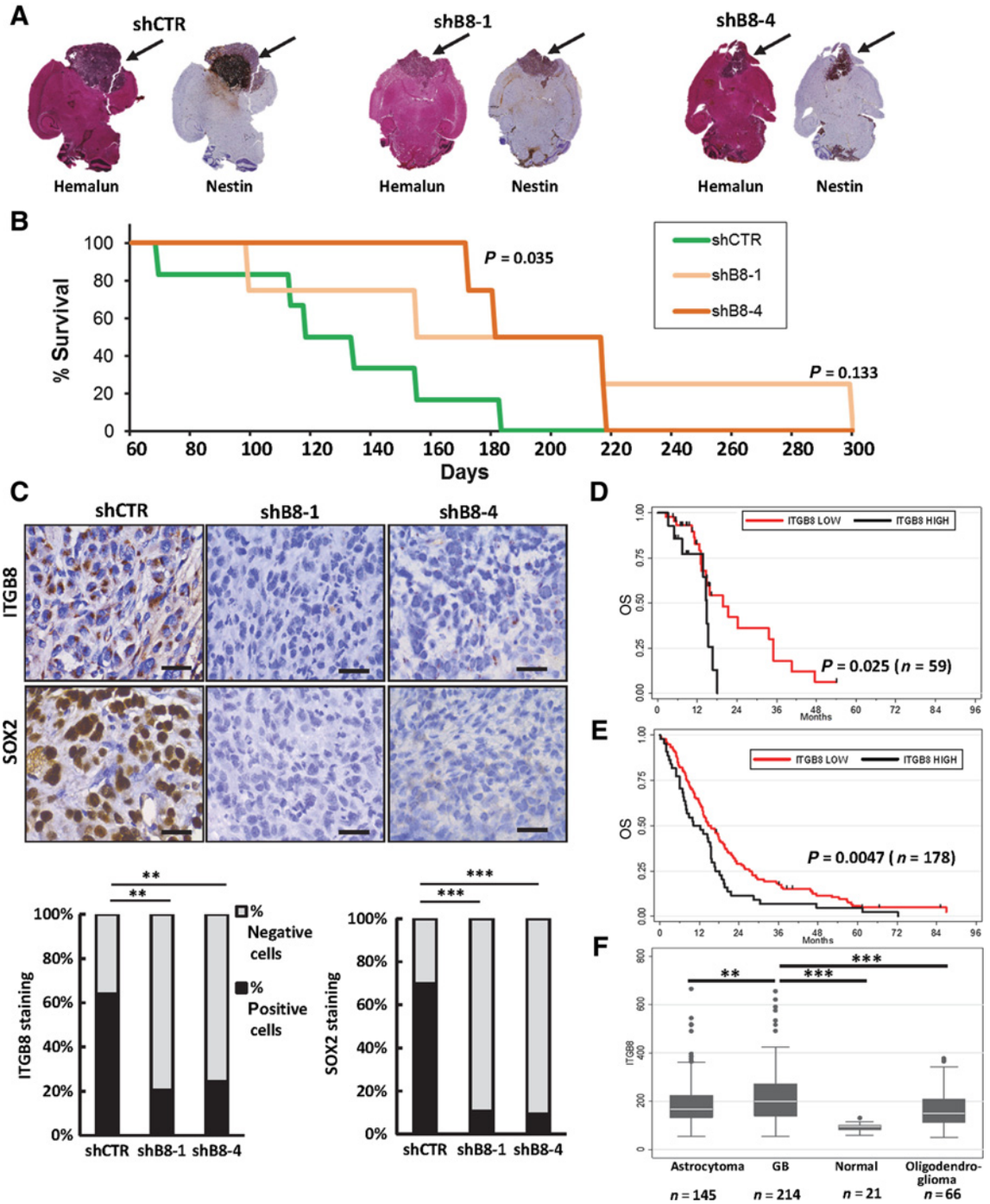

Figure 7.

High ITGβ8 expression is correlated with increased tumorigenesis in xenografted mice and with reduced GB-patient survival. **A–C,** Stably-transfected (shB8-1, shB8-4, or shCTR) SRB1 GICs were dissociated and implanted into the right forebrain of mice. **A,** Representative scans of Hemalun or Nestin staining of mice brains to estimate the presence of an invasive tumor. **B,** Survival curves of mice xenografted with the indicated SRB1 GICs (shB8-1 or shB8-4 or shCTR). Exact *P* values between shB8-1 or shB8-4 groups and the related shCTR group were determined by the log-rank analysis and indicated on the graph. **C,** Immunohistological analysis (top) and quantification (bottom) of ITGβ8 and Sox2 staining within the tumor area of sacrificed mouse. Shown are some representative phase contrast photomicrographs of IHC stainings. Magnification, ×63; scale bar, 50 μm. **, $P \leq 0.01$ and ***, $P \leq 0.001$ compared with the shCTR condition. **D** and **E,** Kaplan–Meier survival plots based on ITGB8 gene expression (**D**) for GB patients in the TCGA cohort ($n = 59$ newly diagnosed primary GB treated with standard chemoradiotherapy) and (**E**) for GB patients in the REMBRANDT cohort ($n = 178$ with survival data). **F,** ITGB8 gene expression plots for astrocytoma, GB, oligodendroglioma patients, or normal tissue from REMBRANDT database. **, $P \leq 0.01$ and ***, $P \leq 0.001$.

differentiation process to lower the high resistance potential of this cell subpopulation (2) and promote GIC cell death.

In that way, we demonstrated here for the first time that, additionally to its role in GIC stemness maintenance, β8 inhibition can induce a significant increase of caspase-dependent GIC apoptosis, with activation of both initiator and effector caspases (Fig. 5). Interestingly, this survival impediment appeared to be potentiated after irradiation, with a notable increase of postmitotic cell death in β8-downregulated GIC (Fig. 6). These results confirm the interest of blocking β8-mediated stemness to favor GIC cell death and hamper their therapeutic resistance. Regarding cancer cell survival impairment, β8 inhibition was shown to induce a potent cell-cycle blockade in lung cancer cells (38) and to decrease hepatic cancer cell survival and proliferation via the inhibition of Survivin and Bcl2, two antiapoptotic proteins, and via the impairment of the TGFβ/Smad pathway (39). Focusing on apoptosis, β8 was notably associated to protection of Oligodendrocytic Progenitor Cells from H_2O_2-induced cell death in response to high levels of Osteopontin (OPN), a secreted ECM phosphoprotein (40). Because OPN, a candidate ligand for αvβ8 (41), was described as a major actor for GIC stemness, GB cell dedifferentiation and tumorigenesis (42–44), and GB cell radioresistance (45), it would be of interest to decipher the OPN role in the β8-induced molecular mechanisms to sustain GIC survival and stemness. Another thing to consider is the role of Survivin in β8-induced GIC stemness, viability, and resistance, because we and other demonstrated that this protein, markedly overexpressed in GIC, is involved in GB cell dedifferentiation, radioresistance, and faster recurrence (18). Finally, a particular focus is required on the TGFβ role in β8-mediated GIC survival and resistance. Indeed, this paracrine and autocrine pathway, notably activated via αvβ8-binding to latent TGFβ complex, was shown to sustain GIC radioresistance (46) as well as to promote proliferation, invasion, angiogenesis, stemness, resistance, and tumor initiation/progression in GB (47). Manifestly, signaling pathways associated to β8 effects on GIC stemness, survival, and resistance remain to be explored, particularly the identification of ligands which may interact with β8 to transduce signals and modulate GIC biological processes and functions.

Growing evidences point out ITGβ8 as a specific GIC marker and highlight its role in GIC stemness, survival, and resistance. We therefore propose this integrin as a new potential therapeutic target in GB, because β8 appears to act by various mechanisms to alter GIC functions, aggressiveness, and radioresistance. Considering the fact that (i) the clinical targeting of αvβ3/αvβ5 by Cilengitide recently failed in GB patients (10) and that (ii) the GIC subpopulation, proved to greatly support the quick recurrence of GB after treatment, was described to express low and variable expression levels of αvβ3/αvβ5 [our present results and (ref. 9)], it is worth hypothesizing that the targeting of β8 in this specific GIC subpopulation could, in combination with radio/chemotherapy, significantly impede the development of these aggressive brain tumors. Significant effort is then required to develop specific β8 inhibitors, already tested at the preclinical level for tumor immunotherapy (48), and to set up new combined therapeutic strategies for GB outcome improvement.

Disclosure of Potential Conflicts of Interest

No potential conflicts of interest were disclosed.

Authors' Contributions

Conception and design: L. Malric, S. Monferran, P. Dahan, S. Boyrie, E. Cohen-Jonathan Moyal, C. Toulas, A. Lemarié

Development of methodology: L. Malric, C. Delmas, F. Arnauduc, P. Dahan, S. Boyrie, A. Lemarié

Acquisition of data (provided animals, acquired and managed patients, provided facilities, etc.): L. Malric, S. Monferran, C. Delmas, F. Arnauduc, P. Dahan, V. Lubrano, D. Ferreira Da Mota, S. Evrard, A. Lemarié

Analysis and interpretation of data (e.g., statistical analysis, biostatistics, computational analysis): L. Malric, S. Monferran, C. Delmas, F. Arnauduc, P. Dahan, S. Boyrie, J. Gilhodes, T. Filleron, A. Lemarié

Writing, review, and/or revision of the manuscript: L. Malric, S. Monferran, F. Arnauduc, S. Boyrie, V. Lubrano, J. Gilhodes, T. Filleron, A. Kowalski-Chauvel, E. Cohen-Jonathan Moyal, C. Toulas, A. Lemarié

Administrative, technical, or material support (i.e., reporting or organizing data, constructing databases): L. Malric, C. Delmas, P. Deshors, D. Ferreira Da Mota, A. Siegfried, S. Evrard, A. Lemarié

Study supervision: L. Malric, A. Kowalski-Chauvel, E. Cohen-Jonathan Moyal, C. Toulas, A. Lemarié

Acknowledgments

We would like to thank Emmanuelle Uro-Coste and Monique Courtade-Saïdi at the IUCT-oncopole Anatomopathology service, Jean-José Maoret and Fréderic Martins at the Toulouse GeT Platform, Manon Farcé (INSERM U1037, Technology Cluster) for her technical assistance on the FACS sorting, and Julie Sesen and Nicolas Skuli for their scientific inputs. We also want to acknowledge the Institut Claudius Regaud and GRICR, RITC Foundation (Stemri), INSERM, the Cancéropôle Grand Sud-Ouest (A. Lemarié), the Association pour la Recherche sur les Tumeurs Cérébrales (A. Lemarié and L. Malric), and the THE program from Plan Cancer 2016 (MoGlimaging). L. Malric and S. Boyrie were supported by a PhD fellowship from Plan Cancer/ITMO and P. Dahan and P. Deshors by a government PhD fellowship.

This work was supported by Recherche Innovation Thérapeutique Cancérologie (RITC), the THE program (INSERM, INCa, Plan cancer), the Groupe de Recherche de l'Institut Claudius Regaud (GRICR), the Cancéropôle Grand Sud-Ouest (GSO), and the Association pour la Recherche sur les Tumeurs Cérébrales (ARTC).

The costs of publication of this article were defrayed in part by the payment of page charges. This article must therefore be hereby marked *advertisement* in accordance with 18 U.S.C. Section 1734 solely to indicate this fact.

Received April 19, 2018; revised July 13, 2018; accepted September 12, 2018; published first September 28, 2018.

References

1. Weller M, van den Bent M, Hopkins K, Tonn JC, Stupp R, Falini A, et al. EANO guideline for the diagnosis and treatment of anaplastic gliomas and glioblastoma. Lancet Oncol 2014;15:e395–403.
2. Lathia JD, Mack SC, Mulkearns-Hubert EE, Valentim CL, Rich JN. Cancer stem cells in glioblastoma. Genes Dev 2015;29:1203–17.
3. Takada Y, Ye X, Simon S. The integrins. Genome Biol 2007;8:215.
4. Hehlgans S, Haase M, Cordes N. Signalling via integrins: implications for cell survival and anticancer strategies. Biochim Biophys Acta 2006;1775:163–80.
5. Malric L, Monferran S, Gilhodes J, Boyrie S, Dahan P, Skuli N, et al. Interest of integrins targeting in glioblastoma according to tumor heterogeneity and cancer stem cell paradigm: an update. Oncotarget 2017;8:86947–68.
6. Nakada M, Nambu E, Furuyama N, Yoshida Y, Takino T, Hayashi Y, et al. Integrin alpha3 is overexpressed in glioma stem-like cells and promotes invasion. Br J Cancer 2013;108:2516–24.
7. Lathia JD, Gallagher J, Heddleston JM, Wang J, Eyler CE, Macswords J, et al. Integrin alpha 6 regulates glioblastoma stem cells. Cell Stem Cell 2010;6:421–32.

8. Haas TL, Sciuto MR, Brunetto L, Valvo C, Signore M, Fiori ME, et al. Integrin alpha7 Is a Functional Marker and Potential Therapeutic Target in Glioblastoma. Cell Stem Cell 2017;21:35–50.
9. Roth P, Silginer M, Goodman SL, Hasenbach K, Thies S, Maurer G, et al. Integrin control of the transforming growth factor-beta pathway in glioblastoma. Brain 2013;136:564–76.
10. Stupp R, Hegi ME, Gorlia T, Erridge SC, Perry J, Hong YK, et al. Cilengitide combined with standard treatment for patients with newly diagnosed glioblastoma with methylated MGMT promoter (CENTRIC EORTC 26071-22072 study): a multicentre, randomised, open-label, phase 3 trial. Lancet Oncol 2014;15:1100–8.
11. Lakhe-Reddy S, Li V, Arnold TD, Khan S, Schelling JR. Mesangial cell alphavbeta8-integrin regulates glomerular capillary integrity and repair. Am J Physiol Renal Physiol 2014;306:F1400–9.
12. Mobley AK, Tchaicha JH, Shin J, Hossain MG, McCarty JH. Beta8 integrin regulates neurogenesis and neurovascular homeostasis in the adult brain. J Cell Sci 2009;122:1842–51.
13. Riemenschneider MJ, Mueller W, Betensky RA, Mohapatra G, Louis DN. In situ analysis of integrin and growth factor receptor signaling pathways in human glioblastomas suggests overlapping relationships with focal adhesion kinase activation. Am J Pathol 2005;167:1379–87.
14. Lathia JD, Heddleston JM, Venere M, Rich JN. Deadly teamwork: neural cancer stem cells and the tumor microenvironment. Cell Stem Cell 2011;8:482–5.
15. Reyes SB, Narayanan AS, Lee HS, Tchaicha JH, Aldape KD, Lang FF, et al. alphavbeta8 integrin interacts with RhoGDI1 to regulate Rac1 and Cdc42 activation and drive glioblastoma cell invasion. Mol Biol Cell 2013;24:474–82.
16. Tchaicha JH, Reyes SB, Shin J, Hossain MG, Lang FF, McCarty JH. Glioblastoma angiogenesis and tumor cell invasiveness are differentially regulated by beta8 integrin. Cancer Res 2011;71:6371–81.
17. Guerrero PA, Tchaicha JH, Chen Z, Morales JE, McCarty N, Wang Q, et al. Glioblastoma stem cells exploit the alphavbeta8 integrin-TGFbeta1 signaling axis to drive tumor initiation and progression. Oncogene 2017;36:6568–80.
18. Dahan P, Martinez Gala J, Delmas C, Monferran S, Malric L, Zentkowski D, et al. Ionizing radiations sustain glioblastoma cell dedifferentiation to a stem-like phenotype through survivin: possible involvement in radioresistance. Cell Death Dis 2014;5:e1543.
19. Markovics JA, Araya J, Cambier S, Jablons D, Hill A, Wolters PJ, et al. Transcription of the transforming growth factor beta activating integrin beta8 subunit is regulated by SP3, AP-1, and the p38 pathway. J Biol Chem 2010;285:24695–706.
20. Sadok A, Bourgarel-Rey V, Gattacceca F, Penel C, Lehmann M, Kovacic H. Nox1-dependent superoxide production controls colon adenocarcinoma cell migration. Biochim Biophys Acta 2008;1783:23–33.
21. Cancer Genome Atlas Research Network. Comprehensive genomic characterization defines human glioblastoma genes and core pathways. Nature 2008;455:1061–8.
22. Verhaak RG, Hoadley KA, Purdom E, Wang V, Qi Y, Wilkerson MD, et al. Integrated genomic analysis identifies clinically relevant subtypes of glioblastoma characterized by abnormalities in PDGFRA, IDH1, EGFR, and NF1. Cancer Cell 2010;17:98–110.
23. Roos A, Ding Z, Loftus JC, Tran NL. Molecular and microenvironmental determinants of glioma stem-like cell survival and invasion. Front Oncol 2017;7:120.
24. van der Flier A, Sonnenberg A. Function and interactions of integrins. Cell Tissue Res 2001;305:285–98.
25. Bao S, Wu Q, McLendon RE, Hao Y, Shi Q, Hjelmeland AB, et al. Glioma stem cells promote radioresistance by preferential activation of the DNA damage response. Nature 2006;444:756–60.
26. Gouaze-Andersson V, Delmas C, Taurand M, Martinez-Gala J, Evrard S, Mazoyer S, et al. FGFR1 induces glioblastoma radioresistance through the PLCgamma/Hif1alpha pathway. Cancer Res 2016;76:3036–44.
27. Louis DN, Perry A, Reifenberger G, von Deimling A, Figarella-Branger D, Cavenee WK, et al. The 2016 World Health Organization Classification of Tumors of the Central Nervous System: a summary. Acta Neuropathol 2016;131:803–20.
28. Chao C, Carmical JR, Ives KL, Wood TG, Aronson JF, Gomez GA, et al. CD133+ colon cancer cells are more interactive with the tumor microenvironment than CD133- cells. Lab Invest 2012;92:420–36.
29. Patel AP, Tirosh I, Trombetta JJ, Shalek AK, Gillespie SM, Wakimoto H, et al. Single-cell RNA-seq highlights intratumoral heterogeneity in primary glioblastoma. Science 2014;344:1396–401.
30. Schittenhelm J, Klein A, Tatagiba MS, Meyermann R, Fend F, Goodman SL, et al. Comparing the expression of integrins alphavbeta3, alphavbeta5, alphavbeta6, alphavbeta8, fibronectin and fibrinogen in human brain metastases and their corresponding primary tumors. Int J Clin Exp Pathol 2013;6:2719–32.
31. Weller M, Nabors LB, Gorlia T, Leske H, Rushing E, Bady P, et al. Cilengitide in newly diagnosed glioblastoma: biomarker expression and outcome. Oncotarget 2016;7:15018–32.
32. Janouskova H, Maglott A, Leger DY, Bossert C, Noulet F, Guerin E, et al. Integrin alpha5beta1 plays a critical role in resistance to temozolomide by interfering with the p53 pathway in high-grade glioma. Cancer Res 2012;72:3463–70.
33. Virga J, Bognar L, Hortobagyi T, Zahuczky G, Csosz E, Kallo G, et al. Prognostic role of the expression of invasion-related molecules in glioblastoma. J Neurol Surg A Cent Eur Neurosurg 2017;78:12–9.
34. Ducassou A, Uro-Coste E, Verrelle P, Filleron T, Benouaich-Amiel A, Lubrano V, et al. alphavbeta3 Integrin and fibroblast growth factor receptor 1 (FGFR1): Prognostic factors in a phase I-II clinical trial associating continuous administration of Tipifarnib with radiotherapy for patients with newly diagnosed glioblastoma. Eur J Cancer 2013;49:2161–9.
35. Ortensi B, Setti M, Osti D, Pelicci G. Cancer stem cell contribution to glioblastoma invasiveness. Stem Cell Res Ther 2013;4:18.
36. Mehta S, Lo Cascio C. Developmentally regulated signaling pathways in glioma invasion. Cell Mol Life Sci 2017;75:385–402.
37. Mertens-Walker I, Fernandini BC, Maharaj MS, Rockstroh A, Nelson CC, Herington AC, et al. The tumour-promoting receptor tyrosine kinase, EphB4, regulates expression of Integrin-beta8 in prostate cancer cells. BMC Cancer 2015;15:164.
38. Xu Z, Wu R. Alteration in metastasis potential and gene expression in human lung cancer cell lines by ITGB8 silencing. Anat Rec 2012;295:1446–54.
39. Wang WW, Wang YB, Wang DQ, Lin Z, Sun RJ. Integrin beta-8 (ITGB8) silencing reverses gefitinib resistance of human hepatic cancer HepG2/G cell line. Int J Clin Exp Med 2015;8:3063–71.
40. Mazaheri N, Peymani M, Galehdari H, Ghaedi K, Ghoochani A, Kiani-Esfahani A, et al. Ameliorating effect of osteopontin on H2O2-induced apoptosis of human oligodendrocyte progenitor cells. Cell Mol Neurobiol 2017;38:891–9.
41. Ozawa A, Sato Y, Imabayashi T, Uemura T, Takagi J, Sekiguchi K. Molecular basis of the ligand binding specificity of alphavbeta8 integrin. J Biol Chem 2016;291:11551–65.
42. Friedmann-Morvinski D, Bhargava V, Gupta S, Verma IM, Subramaniam S. Identification of therapeutic targets for glioblastoma by network analysis. Oncogene 2016;35:608–20.
43. Pietras A, Katz AM, Ekstrom EJ, Wee B, Halliday JJ, Pitter KL, et al. Osteopontin-CD44 signaling in the glioma perivascular niche enhances cancer stem cell phenotypes and promotes aggressive tumor growth. Cell Stem Cell 2014;14:357–69.
44. Lamour V, Henry A, Kroonen J, Nokin MJ, von Marschall Z, Fisher LW, et al. Targeting osteopontin suppresses glioblastoma stem-like cell character and tumorigenicity in vivo. Int J Cancer 2015;137:1047–57.
45. Henry A, Nokin MJ, Leroi N, Lallemand F, Lambert J, Goffart N, et al. New role of osteopontin in DNA repair and impact on human glioblastoma radiosensitivity. Oncotarget 2016;7:63708–21.
46. Anido J, Saez-Borderias A, Gonzalez-Junca A, Rodon L, Folch G, Carmona MA, et al. TGF-beta receptor inhibitors target the CD44(high)/Id1(high) glioma-initiating cell population in human glioblastoma. Cancer Cell 2010;18:655–68.
47. Joseph JV, Balasubramaniyan V, Walenkamp A, Kruyt FA. TGF-beta as a therapeutic target in high grade gliomas - promises and challenges. Biochem Pharmacol 2013;85:478–85.
48. Stockis J, Lienart S, Colau D, Collignon A, Nishimura SL, Sheppard D, et al. Blocking immunosuppression by human Tregs in vivo with antibodies targeting integrin alphaVbeta8. Proc Natl Acad Sci U S A 2017;114:E10161–8.